STRENGTH OF END-NOTCHED WOOD BEAMS: A CRITICAL FILLET HOOP STRESS APPROACH

Greg C. Foliente
Graduate Project Assistant

and

Thomas E. McLain
Professor
Department of Wood Science and Forest Products
Virginia Polytechnic Institute and State University
Blacksburg, VA 24061

(Received March 1991)

ABSTRACT

An equation for predicting the strength of wood beams with end notches on the tension side (Tension-side End Notches or TEN) was derived using a critical fillet hoop stress (CFHS) theory. The equation combines the results of finite element and statistical analyses of 690 different TEN beam configurations and experimental tests of 362 full-size beams. It accounts for the effects of loading type, end support and beam and notch geometry variables such as beam height, fractional notch depth, radius, and notch location. The effect of span-to-depth ratio is implicit to the model. Notched beam strength is represented by a material parameter, κ, which can be obtained from notched beam tests. The equation is applicable to both filleted and sharp-cornered notches. An effective radius, R_e, which models the effect of a sharp-cornered notch, was determined and confirmed for two wood materials. A method of determining R_e for other materials was established. The results of this study can be used to set new design criteria for the strength of notched wood beams.

Keywords: Beam strength, notch, wood beam, wood design, end effects.

INTRODUCTION

Wood beams are notched in construction to bring top surfaces of floors and roofs to desired levels, or to provide necessary clearance or fit to support or framing conditions. Notching the ends of a wood beam on the tension face severely reduces beam strength beyond that due to a reduction in net section because of stress concentration at the notch root. Researchers such as Murphy (1978), Gustafsson (1988), Walsh (1972), and Leicester and Poynter (1979) have characterized this as a fracture phenomenon and provide limited prediction equations. Most building codes, standards, and design guides recommend avoiding notches (USDA 1987; NFPA 1986; AITC 1985; Mettem 1986; CSA 1989). Current U.S. design practice is based on unpublished empirical work by Scholten (1935) and does not behaviorally conform with the research results mentioned above. Foliente and McLain (1991) demonstrated that U.S. design recommendations are nonconservative for some notch geometries.

The stresses at a notch root in an orthotropic wood beam are complex, and the combination of stresses that initiates failure or crack propagation is unknown. Gerhardt (1984a, b) successfully modeled the stresses at the filleted notch of oak pallet stringers using a hybrid finite element (FE) model. He found that failure was initiated when the maximum hoop stress at the notch fillet reached a critical value (referred to here as the critical fillet hoop stress

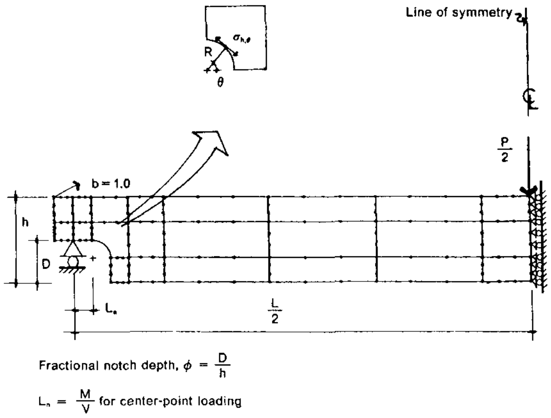

FIG. 1. FE model of wood beam with TEN.

or CFHS theory). Fillet hoop stress, $\sigma_{h,\theta}$, is the "non-zero principal stress acting on the free surface of a filleted notch corner at an angle θ from the horizontal" (Zalph 1989), as shown in Fig. 1. Gerhardt (1984a) found that maximum hoop stress could be predicted by

$$\sigma_{h,max} = \left(\frac{6M}{bh^2}\right) f_1 + \left(\frac{6V}{bh}\right) f_2 \qquad (1)$$

where

- $\sigma_{h,max}$ = maximum hoop stress at critical notch root,
- M, V = resultant bending moment and shear, respectively, at the critical notch root,
- b, h = beam width and beam height, respectively
- f_1 = moment term apparent stress concentration factor,
- f_2 = shear term apparent stress concentration factor.

Abou-Ghaida and Gopu (1984) confirmed Gerhardt's work for tension-side interior notches and supported the CFHS theory. Zalph (1989) and Zalph and McLain (1992) tested the general applicability of the theory for a wide range of tension notch and beam geometries with an extensive analytical and experimental study. They developed a closed-form equation that predicts the flexure strength of these notched beams.

Abou-Ghaida and Gopu (1984), however, found that Eq. (1) seriously underestimates the hoop stress at end notches on the tension face of a beam (Tension-side End Notches or TEN). We hypothesize that Gerhardt's and Zalph's work was influenced by the dominant moment term in Eq. (1), whereas for TEN beams the shear term is more critical.

The objectives of this research were to (a) develop a closed-form prediction equation for the maximum hoop stress in a TEN wood beam considering notch, beam, loading, and material variables, and (b) experimentally assess the validity of the CFHS theory to model failure in TEN wood beams, including those with sharp notches.

If CFHS theory is sufficiently accurate, then it may be used to develop new design criteria for the strength of end-notched beams. Designers and engineers are currently left without adequate guidance when designing TEN wood beams.

CLOSED-FORM EQUATIONS

Finite element model

An end-notched wood beam, Fig. 1, is characterized by its span (L), beam width (b) and depth (h), notch depth (D), fractional notch depth or ratio D/h (ϕ), fillet radius (R), notch length (L_n), loading condition (M/V), and elastic parameters. Gerhardt's (1983, 1984a, b) FE program was used to model beams with different combinations of these parameters. Cubic isoparametric quadrilateral plane elements were used except at the notch root, which was modeled with a planar hybrid fillet element. Note the exploitation of symmetry in Fig. 1. Characteristic details of these elements were published by Gerhardt (1983, 1984a, b). The following were assumed: (a) plane stress loading, (b) orthotropic linear elastic material, with (c) principal material axes aligned with beam axes (i.e., no slope-of-grain).

All analyses were run on an IBM 3090 mainframe computer. A single output file—containing the hoop stresses, $\sigma_{h,\theta}$, given at 1° increments from 0° to 90° with respect to the horizontal axis, the maximum hoop stress,

$\sigma_{h,max}$, its angle of occurrence, θ_{max}, the maximum displacement and its node location—was received from the program.

Derivation

Analysis.—It is hypothesized that a crack-initiated mode of failure in a TEN wood beam results when the maximum hoop stress at the notch root exceeds a critical level. Equation (1) may be normalized and rearranged to yield

$$\mathrm{ShCF} = \frac{\sigma_{h,max}}{\left(\frac{6V}{bh}\right)} = f_1\left(\frac{M}{V}\right)\frac{1}{h} + f_2 \quad (2)$$

where

ShCF = normalized hoop stress or "Shear Concentration Factor,"

$\frac{M}{V}$ = ratio of applied moment to applied shear at the notch root location.

The moment and shear functions, f_1 and f_2, will contain terms related to some or all of the following: L, h, D, ϕ, R, L_n, M/V and material properties.

For orthotropic wood (where E is Young's moduli, G is shear moduli, x corresponds to the longitudinal axis and y to a transverse axis—radial and tangential properties assumed equal), the ratios E_x/E_y and E_x/G_{xy} influence beam displacements and stresses and specifically, maximum hoop stress $\sigma_{h,max}$ using Gerhardt's (1984a) model. For the present study, the elastic property sets shown in Table 1 were chosen to model a wide range of wood species. Poisson's ratio, ν_{xy}, was set constant at 0.40 as Gerhardt (1984a) found that ν_{xy} had a negligible influence on calculated stresses and displacements.

Beam geometry in the FE analysis was described by variable h, a fixed L and a unit width. Notch geometry variables were R and ϕ (or ratio D/H). Notch length, L_n, identifies the location of the notch root relative to the support. For center-point loading, L_n is also equal to the ratio of M/V at the notch root.

TABLE 1. *Elastic property (EP) sets considered in the FE analysis of TEN wood beams. Poisson's ratio was constant at 0.40.*

		Orthotropy ratios			
EP set	Designation	$\frac{E_x}{G_{xy}}$	$\frac{E_x}{E_y}$	$\frac{E_y}{G_{xy}}$	E_x ($\times 10^6$ psi)
A	G11-E13	11	13	0.846	1.3
B	G17-E17	17	17	1.000	1.7
C	G27-E21	27	21	1.286	1.7
D	G11-E17	11	17	0.647	1.7
E	G27-E17	27	17	1.588	1.7

This loading type was selected for convenience.

A full factorial numerical analysis was performed using the variables shown below:

variable	levels
h (in.)	3.50, 4.71, 7.125, 10.75
ϕ	0.10, 0.35, 0.52, 0.60
R (in.)	0.1875, 0.344, 0.50
M/V (in.)	1.0, 6.5, 12.0
material	A, B, C, D, E (see Table 1)

The ranges of geometry variables were chosen based on preliminary studies and practicality. Beam span was 42 in. and total beam length, 48 in. With each elastic property (EP) set, six geometric cases were not analyzed because R > D. Consequently, a total of 138 ShCF values per EP set and a grand total of 690 different notched beams were analyzed numerically. Although the study did not include span-to-depth, L/h, as an explicit variable, it covered cases where L/h ranged from 3.91 to 12.00.

Equation (2) is linear with an intercept of f_2 and a slope of $(1/h)f_1$, where $f_2 = f_2(\text{EP set}, \phi, R, h)$ and $f_1 = f_1(\text{EP set}, \phi, R, h)$. Linear regressions with FE-derived ShCF and notch location M/V as dependent and independent variables, respectively, were made for all combinations of ϕ, R, and h for each EP set. This resulted in 46 values of f_1 and f_2 for each EP set. The results showed high linearity with coefficients of determination (r^2) values generally exceeding 0.999. This supports the use of Eq. (1) for hoop stress or ShCF prediction. Analyses ranged from shear-dominated cases (M/V

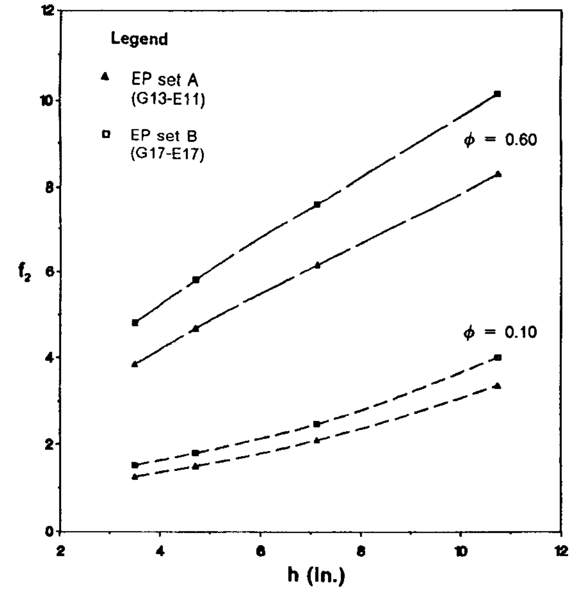

FIG. 2. Influence of beam height on moment term factor, f_2, for EP sets A and B.

= 1.00 in.) to moment-dominated cases (M/V = 12.0 in.).

Elastic property factors.—The effect of elastic properties on maximum hoop stress was separated from that of geometric variables by

$$f_1 = \mu_1 F_1 \quad \text{and} \quad f_2 = \mu_2 F_2 \qquad (3)$$

where

μ_1, μ_2 = parameters that are solely dependent on elastic properties

F_1, F_2 = material-independent beam and notch geometry functions.

Relationships between the derived factors (f_1 and f_2) and geometric variables were extensively examined. A typical plot is shown in Fig. 2. The consistent parallel nature of the lines representing different EP sets in all studies confirmed the assumption of material invariance in the functions F_1 and F_2 of Eq. (3). Material factors μ_1 and μ_2 were determined from the f_1 and f_2 values calculated for each EP set. The material factors were normalized relative to a baseline EP set B (G17-E17), where μ_1 and μ_2 are set to unity and $f_1 = F_1$, $f_2 = F_2$; see Table 2.

Expressions for F_1 and F_2.—The 46 values of f_1 and f_2 from EP set G17-E17 were fit with over 20 candidates of linear and nonlinear models using the Statistical Analysis System (SAS Institute 1985). Recall that $f_1 = F_1$, $f_2 = F_2$, and $\mu_1 = \mu_2 = 1$ for this data set. The models were evaluated using: (1) r^2 and Mallows' Cp statistic, (2) a visual check of residuals, and (3) the computed relative prediction error, FERR, for every observation [(actual − predicted)/(actual) × 100%]. The mean FERR was calculated and the overall FERR distribution plotted for visual evaluation. The FERR evaluation process was given greater weight over other criteria because the end result will be primarily used for prediction purposes.

The best fitting moment term function, F_1, was found to be

$$F_1 = \frac{1}{0.159 - 0.213\phi + 0.187\left(\dfrac{R}{D}\right)}. \qquad (4)$$

This form has a mean FERR of 1% (overprediction) with standard deviation of 8.2%.

TABLE 2. *Material factors calibrated from the baseline EP set G17-E17 (from 46 observations).*

	Orthotropy ratios			Material factor			
EP set	$\frac{E_x}{G_{xy}}$	$\frac{E_x}{E_y}$	$\frac{E_y}{G_{xy}}$	μ_1	μ_2	$\mu = \frac{\mu_2}{\mu_1}$	Predicted μ_p[1]
A	11	13	0.846	0.915	0.818	0.894	0.894
B	17	17	1.000	1.000	1.000	1.000	1.006
C	27	21	1.286	1.112	1.246	1.121	1.118
D	11	17	0.647	0.930	0.939	1.010	1.006
E	27	17	1.588	1.110	1.150	1.036	1.006

[1] From $\mu_p = 0.530 + 0.028\left(\frac{E_x}{G_{xy}}\right)$; (coeff. of determination, $r^2 = 0.971$).

TABLE 3. *Error in predicting ShCF using Eq. (8).*

	Relative prediction error, ShCFERR (%)			
EP set	Mean[1]	Std. deviation	Maximum over-prediction	Maximum under-prediction
A	0.67	4.84	12.7	13.9
B	0.66	4.79	15.2	11.9
C	0.58	5.26	17.0	12.5
D	0.54	5.29	15.6	14.8
E	0.40	5.62	18.9	12.2

[1] Positive sign means on the underprediction side.

Maximum over- and underpredictions of actual values were 25.3% and 11.8%, respectively.

For the shear term factor, the best fit function was

$$F_2 = 1.464\phi^{0.712}R^{-0.418}h^{(0.847 - 0.316\phi)}. \quad (5)$$

This equation overpredicted the actual values for two cases out of 46 by over 12% and underpredicted another two cases by over 10%. FERRs for all other geometry cases (42 out of 46), however, fell within the tight range of ±5.9% of mean zero.

Closed-form equation.—Substituting Eq. (3) into (2) and rearranging,

$$\frac{\sigma_{h,max}}{\mu_1} = \left(\frac{6V}{bh}\right)\left[F_1\left(\frac{M}{V}\right)\frac{1}{h} + \frac{\mu_2}{\mu_1}F_2\right]. \quad (6)$$

Let $K = \frac{\sigma_{h,max}}{\mu_1}$ and $\mu = \frac{\mu_2}{\mu_1}$, then

$$\frac{6V}{bh} = \frac{K}{\left[F_1\left(\frac{M}{V}\right)\frac{1}{h} + \mu F_2\right]}. \quad (7)$$

This form is convenient for predicting a critical shear value for a notched beam. K is an experimentally determined material constant. The ratio $\mu = \frac{\mu_2}{\mu_1}$ was approximately linear with orthotropy ratio E_x/G_{xy} (see Table 2). Because E_x/G_{xy} is generally unknown and applicability to all EP sets is desired, μ was set constant at 1.12. Since μ is a multiplier to the shear term in Eq. (6), its effect is negligible for moment-dominated cases. It does provide additional safety in some materials for shear-dominated cases, e.g., notch root at or close to the support.

Evaluation.—Substituting (3), (4) and (5) into (2) and rearranging,

$$\text{ShCF} = \frac{\sigma_{h,max}}{\left(\frac{6V}{bh}\right)} = \mu_1\left[\frac{1}{0.159 - 0.213\phi + 0.187\left(\frac{R}{D}\right)}\right]\cdot\left(\frac{M}{V}\right)\left(\frac{1}{h}\right) + \mu_2 1.464\phi^{0.712}R^{-0.418}h^{(0.847-0.316\phi)} \quad (8)$$

where μ_1 and μ_2 are in Table 2. This equation was used to predict ShCF for all geometries considered in the FE study. These were compared to actual ShCFs obtained from FE analysis (138 comparisons per EP set). Relative prediction error shown in Table 3 was computed as ShCFERR = (actual − predicted)/(actual) × 100%.

These results show that the closed-form expression accurately predicts the maximum hoop stress found from FE analysis for a range of practical cases. With this equation, the maximum hoop stress of a specific end-notched wood beam geometry may be estimated without resorting to the use of finite element analysis.

EXPERIMENTAL STUDIES

The experimental plan tested the ability of CFHS-based Eq. (7) to predict the strength of wood beams with a practical range of TEN configurations. Specifically, it tested the assumption that geometry and material effects are separable, i.e., that K is geometry-independent. Other experimental objectives were to assess (a) whether K is related to material properties such as specific gravity, block shear strength, and/or perpendicular-to-grain tensile strength, and (b) if sharp-cornered notches can be practically modeled as filleted with an effective radius, R_e.

Materials.—Two materials were selected to represent anatomically different softwood and hardwood species groups: southern yellow pine (*Pinus* spp.) and yellow poplar (*Liriodendron tulipifera*). Kiln-dried pine lumber with minimum defects was purchased from a local lumber yard. Bending specimens measuring 1.5 × 3.5 × 48 in. and 1.5 × 9 × 48 in. were cut from the nominal 2 × 8 in. and 2 × 10 in. materials, respectively. All specimens were free of defects in the notch area.

Most kiln-dried poplar was obtained from a local mill. Nearly clear beams, measuring 1.5 × 3.5 × 47 in. and 1.5 × 9 × 47 in., were cut from 2 × 10 in. boards. For the effective radius substudy, 15 pieces of 1.5 × 3.5 × 48 in. lumber were taken from the stock used in another study.

Filleted TEN beam study.—All variables considered in the FE study were also considered in this experimental study. These include beam height h, fractional notch depth ϕ, radius R, notch location M/V, and material. A randomized complete block design was used with geometry variables contained in a block and each block representing a species group. The levels of the experimental variables are given below. M/V, expressed as notch location, was measured from the center of a 2 in.-wide aluminum block support. Thus, a notch at the support has M/V = 1.0 in.

variable	levels
h (in.)	3.5, 9.0
ϕ	0.20, 0.50
R (in.)	0.25, 0.50
M/V (in.)	1.0, 10.0

Each cell contained four replicates, except for two out of the sixteen cells per block. These cells each contained 6 to 9 additional samples collected in the sharp-cornered TEN beam study, discussed below. The total number of bending tests performed on filleted TEN beams was 158 (2h × 2ϕ × 2R × 2M/V × 2sp. × 4 + 30 = 128 + 30 = 158).

Beam width, b, was constant at approximately 1.5 in. and beam span, L, was maintained at 42 in.; this gave span-to-depth (L/h) ratios of 12.0 and 4.7 for h of 3.5 and 9 in., respectively.

Sharp-cornered TEN beam substudy.—Notch location, M/V, and fractional notch depth, ϕ, were kept constant at 1.0 in. and 0.50, respectively. Most TEN cases in construction have M/V around 1.0 in. Zalph (1989) did not find any conclusive evidence of an effect of ϕ on the value of R_e for interior notches.

Using pine and poplar materials, the following geometry variables were first studied:

variable	levels
h (in.)	3.5. 9.0
R (in.)	0, 0.25

The number of specimens per cell varied depending on the availability of materials. A total of 33 sharp-cornered TEN pine beams (18 for h = 3.5 in. and 15 for h = 9.0 in.) and 25 sharp-cornered poplar beams (16 for h = 3.5 in. and 9 for h = 9.0 in.) were prepared. The filleted counterparts (total of 44) were taken from two cells that correspond to the same geometry for each species in the previously described study.

An additional set of 32 sharp-cornered TEN pine beams with M/V = 1.0 and 10.0 in., ϕ = 0.20 and 0.50, b = 1.5 in. and h = 9.0 in. was later prepared and tested to further confirm earlier results.

Bending tests.—All beams were tested in center-point loading using an MTS servohydraulic testing machine under deformation control at 0.10 in./min. Lateral support at midspan was provided for the 9.0 in.-deep beams. Beam center deflection was sensed using a linear variable differential transformer (LVDT) attached to a yoke system similar to that in ASTM D-198 (American Society for Testing and Materials 1988). (See Fig. 3.) Load-deflection (P-Δ) curves were plotted for each specimen.

Support at the notched end was adjusted for each combination of h and ϕ so that all test beams were level before load application. A 2 in.-wide aluminum bearing block was placed

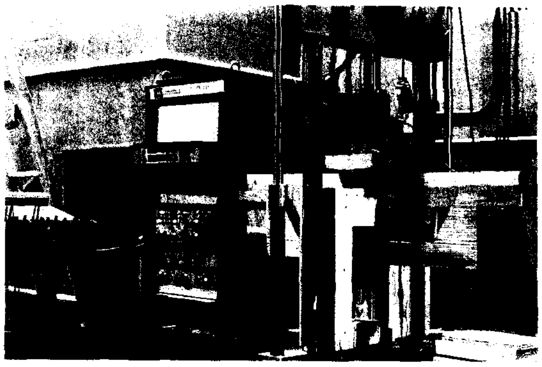

FIG. 3. Test set-up for 9 in.-deep TEN beam.

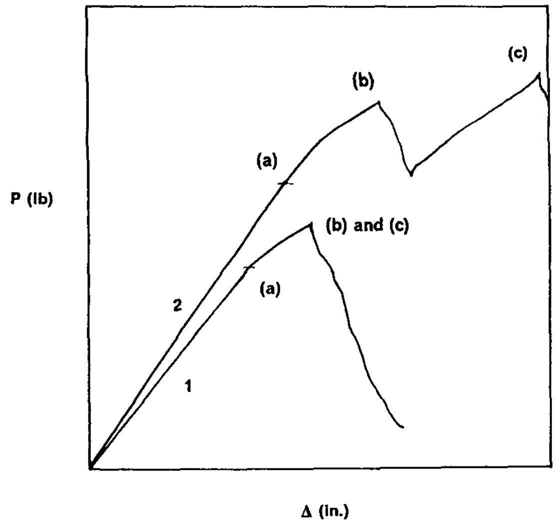

FIG. 4. Schematic diagram of typical load-deflection curves from tests of TEN wood beams—1 for most cases with h = 3.5 in. and 2 for most cases with h = 9.0 in.: (a) proportional limit, (b) major drop, and (c) maximum load.

at the supports to minimize transverse compression. The blocks were attached to tubular steel supports, which were free to roll, thus minimizing axial constraint.

Moisture content and specific gravity.—A representative specimen was cut from the notch root area of all test beams that failed at the notch (61 samples per species). Moisture content and specific gravity were determined using the procedures of ASTM D2395 and D2016 (American Society for Testing and Materials 1988).

For pine, the average MC and SG on ovendry weight and volume basis were 11.4% and 0.54, respectively; for poplar specimens the averages were 7.7% and 0.50, respectively.

Block shear strength.—Shear block samples were cut from test beams at a location free of cracks, knots, and other defects. Totals of 49 pine and 51 poplar samples were obtained. Block shear strength was determined using the procedures of ASTM D143 (American Society for Testing and Materials 1988) except for the reduced specimen size (2 × 1.5 in.) and variable ring orientation. Bendtsen and Porter (1978) found no significant differences between shear strengths of standard and slightly undersized samples.

Perpendicular-to-grain tensile (TPERP) strength.—Tension perpendicular-to-grain (TPERP) samples were taken from a location near that of the shear blocks. Again, ring orientation varied and size was smaller than the ASTM D143 standard. Totals of 49 samples for pine and 50 for poplar were tested using ASTM D143 procedure, and TPERP strength was determined. No adjustments were made for size.

RESULTS AND DISCUSSION

Notched beam strength

The material strength parameter, K, was calculated using

$$K_i = \left(\frac{6V_i}{bh}\right)\left[F_1\left(\frac{M}{V}\right)\frac{1}{h} + \mu F_2\right] \qquad (9)$$

where

i = load level, PL for proportional limit
MAJ for major load drop ($\geq 5\%$)
MAX for maximum load
μ = 1.12 (fixed value from Table 2)
F_1, F_2 = Eqs. (4) and (5), respectively.

The CFHS model is strictly applicable only to notched beam behavior below the beam proportional limit (PL) or before crack initiation (CI). Beam strength beyond PL or CI may not be well modeled because of nonlinear or inelastic behavior.

TABLE 4. *Summary statistics of calculated* K *from experiment.*

Species[1]	M/V (in.)	Load level	n	K Mean (psi)	K Std. deviation	K C.V.[2] (%)
S. pine	1.00	PL	38	5,880	1,420	24.1
		MAJ	39	10,340	2,520	24.3
		MAX	38	10,980	2,720	24.7
	10.00	PL	30	13,900	4,690	33.8
		MAJ	30	18,320	5,340	29.2
		MAX	30	22,480	8,090	36.0
Y. poplar	1.00	PL	34	7,070	2,060	29.1
		MAJ	34	11,040	3,030	27.5
		MAX	33	12,080	3,230	26.7
	10.00	PL	31	14,420	4,190	29.0
		MAJ	32	21,830	3,960	18.1
		MAX	31	27,180	8,840	32.5

[1] The average moisture content of S. pine material was 11.4% and that of Y. poplar material was 7.7%.
[2] C.V., coefficient of variation. C.V. = (std. deviation)/(mean) × 100%.

Zalph (1989) did not find a consistent relationship between PL and CI loads in his work with beams having tension interior notches, and thus he considered only the load at CI. Stieda (1966), however, noted that PL and CI loads always coincided in his tests of small, dry softwood beams. Murphy (1978), with tests of small, dry Douglas-fir beams, also considered PL load as "failure load because it corresponds to crack initiation that precedes visible opening."

In the present study, the visible CI load was observed in the load-deflection (P-Δ) curve to coincide with the first major drop in load (MAJ). This load is defined as the level at which load first drops by 5% or more. For a few beams, the MAJ load occurred at PL, but for most, it occurred beyond PL. Figure 4 shows typical P-Δ curves for wood beams with TEN. Table 4 summarizes test results.

The MAJ load was considered failure because beam behavior after MAJ was unpredictable and highly variable. For TEN beams with h = 3.50 in., $P_{MAJ} = P_{MAX}$ for 81% of pine and 92% of poplar samples. Where h = 9.0 in., this is true only for 38% of pine and 31% of poplar beams. Specimens that continued to bear load after the major load drop acted as prismatic beams with effective depth values controlled by grain slope. These observations of the maximum load were very consistent with those of Stieda (1966), Hirai and Sawada (1979), Murphy (1986), and Gerhardt (1984a). All analyses from here on are, therefore, concerned with MAJ only.

Based on test observations, much of the variability in K_{MAJ} was related to variable ring orientation in the notched beams. This was not quantified.

Geometry effects

Hypothesis testing procedures, described in Foliente (1989), were found to have very low power because of high variances within groups and insufficient sample size. Hence, to assess the geometry independence of K, graphs of cumulative distribution function (cdf) of K within cell groups were compared. If K is independent of geometry, then cdf's from beams with different geometries should be superimposed, essentially showing the same curve.

Figure 5 shows the cdf for K_{MAJ} calculated for poplar beams grouped by M/V and ϕ. It is evident that the effect of ϕ was very small compared to that of M/V. Similar trends were observed when the data were grouped by M/V and h and M/V and R. Plots with comparable data from the pine beam tests showed the same effects. The CFHS theory, while adequate for predicting the effects of geometry variables on

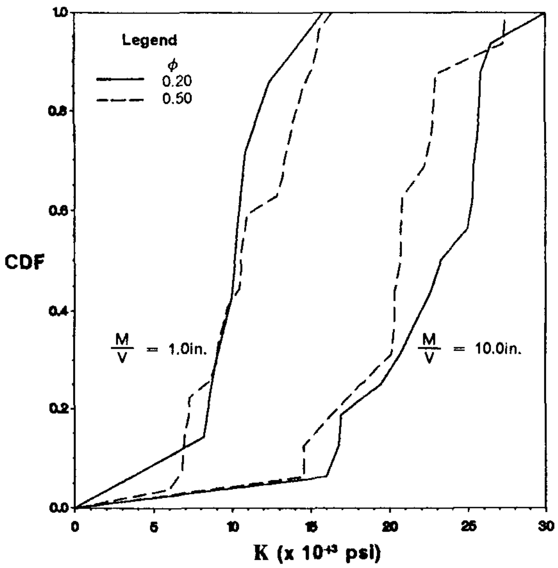

FIG. 5. Cumulative distribution functions of K_{MAJ} for poplar, grouped by M/V and fractional notch depth, ϕ.

strength, may not fully characterize the influence of notch location.

To explore this further, let normalized shear $V^N = V/bh$. This variable allows comparisons of this work with that of other researchers and shows the sensitivity of V^N, as computed from test data, to geometry changes. Ratios of average V^N (or $\bar{V}^N$) at M/V = 1.0 to $\bar{V}^N$ at M/V = 10.0 in. are given in Table 5. These ratios of experimental results are estimates of the true (or population) ratios for the material. Accuracy of the estimates is dependent on sample sizes and variance but these ratios can be compared with theoretical model predictions of V^N.

The sensitivity of model V^N to geometry changes was calculated by fixing material parameters in both TEN and Zalph (1989) equations and calculating V^N's for the selected geometry changes. This was also done with the linear elastic fracture mechanics (LEFM)-based models given by Gustafsson (1988) and the Australian code (SAA 1988). Some results shown in Table 5 indicate that the influence of M/V is not well predicted by any of the LEFM or CFHS models. Changes in other geometry variables (e.g., h, ϕ and R), were predicted reasonably well by most theoretical models. The TEN equation, in particular, gave ratios similar to those from experiment, thus supporting earlier observations made of cdf plots.

The M/V-effect was further examined by physically testing an additional set of matched pine TEN beams with h = 5.50, b = 1.50, D = 1.65 (or ϕ = 0.30), and R = 0.25 in. and M/V varied at 1.0, 5.50 and 10.0 in. (10 beams per M/V for a total of 30 TEN beams). All other test details are the same as described earlier. Average K, shown below, agrees with previous results (see Table 4).

M/V (in.)	$\bar{K}$ (psi)	C.V. (%)
1.0	10,980	28
5.5	15,110	32
10.0	17,850	43

It is interesting to note that the observed increase in V^N (and consequently, K) due to moving the notch root from 10.0 in. to 1.0 in. away from the support was overestimated by both CFHS-based and LEFM-based models. The test data above indicate a slightly curvilinear relationship between K and M/V for notch locations less than or equal to M/V of 10.0 in. The value of K at M/V = 10.0 in., however,

TABLE 5. *Sensitivity of normalized shear capacity to change in notch location.*

		Ratio of $\bar{V}^N$ at M/V = 1.0 in. to $\bar{V}^N$ at M/V = 10.0 in.					
Geometry		Experiment		CFHS theory		LEFM theory[1]	
h (in.)	ϕ	Pine	Poplar	TEN	Zalph	Gus	Aus
3.5	0.20	—	—	4.54	5.41	3.70	3.37
	0.50	2.90	2.67	5.00	6.06	4.35	4.27
9.0	0.20	1.23	1.06	2.25	2.06	2.27	2.10
	0.50	1.61	1.57	2.70	2.25	2.63	2.64

[1] Gus, Gustafsson (1988); Aus, Australian Standard (SAA 1988).

corresponds to that found by Zalph (1989) in beams with a tension interior notch. His results also show that K remained constant as M/V is increased beyond 10.0 in.

The variation in K with notch location for notches close to the support may be explained by Saint-Venant's principle, which states that the stress distribution in an elastic solid is not perturbed by load application, except in the *neighborhood* of the loaded region. This cannot be stated precisely because the principle rests on physical rather than mathematical arguments (Cook and Young 1985). For axially loaded isotropic materials, the characteristic decay length over which end effects are significant is less than or equal to one specimen width. Saint-Venant's principle is thus routinely invoked in neglecting elastic end effects. For axially loaded, highly anisotropic but transversely isotropic materials, however, the characteristic decay length is of the order of several specimen widths (Horgan 1982; Choi and Horgan 1977). With beams, Sandorff (1980) found that the effects of a concentrated transverse load (as that at beam support) on the stress distribution of an isotropic material are highly localized and agree with Saint-Venant's principle; in contrast, the effects in an orthotropic beam extend much further out into the span of the beam.

For the TEN beams in question, stress concentrations arise at the support locations and the notch root. For beam tests where M/V = 1.0 in., the bearing block is adjacent to the notch and the high stresses caused by the support interfered with the free notch stress distribution. The CFHS FE program and fracture mechanics methods did not accurately represent Saint-Venant's end effects. The resulting complex stress distribution was not measured, but its effect is manifested in the decreased experimental value of K for beams with notches at or very close to the support.

Strength prediction equation

Preliminary tests of the M/V-effect indicated that a simple adjustment to Eq. (9) can account for Saint-Venant's end effects in TEN beams. Notch strength parameters for beams with notches within 1.0 in. ≤ M/V ≤ 10.0 in. may be expressed as a function of M/V.

A general strength prediction equation is given as

$$\kappa = A\left(\frac{6M}{bh^2}\right) + B\left(\frac{6V}{bh}\right) \tag{10}$$

where A is is F_1 given in Eq. (4), B is μF_2 or 1.12 F_2 given in Eq. (5) and $\kappa = K - \alpha(\Delta M/V)$. For the case where 1.0 in. ≤ M/V ≤ 10.0 in., $\Delta M/V = 10 - M/V$ and $\alpha = 765$ for pine (obtained from limited tests in this study); where M/V > 10.0 in., $\Delta M/V = 0$ and $\kappa = K$. Further tests are necessary to determine if α is constant for all species.

Sharp-cornered notches—R_e

Most notched beams tested in this substudy (both sharp-cornered or filleted, R = 0.25 in.) had a load-deflection trace with the major load drop coinciding with the maximum load. The data from these tests are used to find an effective (but fictitious) radius, R_e, that allows use of Eq. (10) to predict the strength of sharp-cornered TEN beams.

Equation (10) may be written as

$$\bar{V}^N = \frac{\bar{V}}{bh} = \frac{\bar{\kappa}}{6} g \tag{11}$$

where $\bar{\kappa} = \bar{K} - \alpha(\Delta M/V)$ and

$$g = \frac{1}{\left[F_1\left(\frac{M}{V}\right)\frac{1}{h} + \mu F_2\right]}. \tag{12}$$

The ratio of normalized shear strengths of sharp and filleted TEN beams is

$$\frac{\bar{V}^N_{(R=0)}}{\bar{V}^N_{(R=0.25)}} = \frac{\frac{\bar{\kappa}}{6} g_{R_e}}{\frac{\bar{\kappa}}{6} g_{(R=0.25)}}. \tag{13}$$

Rearranging,

$$g_{R_e} = \left[\frac{\bar{V}^N_{(R=0)}}{\bar{V}^N_{(R=0.25)}}\right] g_{(R=0.25)}. \tag{14}$$

TABLE 6. *Effective radius, R_e, to model sharp-cornered end notches, derived for $M/V = 1.0$ in. and $\phi = 0.50$ by Eq. (14).*

Species	h (in.)	R = 0		R = 0.25 in.		R_e (in.)
		$\bar{V}^N$ (psi)	g	$\bar{V}^N$ (psi)	g	
Pine	3.5	183	0.0903	259	0.1275	0.091
	9.0	132	0.0872	153	0.1012	0.168
Poplar	3.5	163	0.0904	230	0.1275	0.091
	9.0	132	0.0790	169	0.1012	0.128

Everything on the right-hand side of Eq. (14) is known: the bracketed term is a ratio of experimental results and $g_{(R=0.25)}$ is computed using Eq. (12), with nominal values of h, ϕ and D with R = 0.25 in. The computed value of g_{R_e} is equated with Eq. (12) and the radius R_e determined. Calculated R_e are summarized in Table 6. The minimum value was 0.091 in. for both species and in all cases, $0.091 \leq R_e \leq 0.168$. It may be sufficient and convenient to use $R_e = 0.12$ in. to model sharp-cornered notches in beams of dry materials.

Determination of κ

Several linear and nonlinear equations were investigated to relate κ with other material properties (SG, block shear strength and perpendicular-to-grain tensile strength). The nonlinear equations were those linearizable by transformation of either response or predictor variables. The equations had the form similar to those investigated in the FE study. A full prediction model, containing all three material properties as predictor variables, and its subsets were fitted to separate data of pine and poplar. Since the objective was to predict κ from readily known material properties, the evaluation of the models followed the procedure described in the derivation of the theoretical closed-form equation. The relative prediction error in predicting κ was computed as KPERR.

The best prediction models were found to be

$$\kappa = 34{,}822(SG)^{1.04} \quad \text{for pine}$$
$$(r^2 = 0.27 \text{ for transformed linear model})$$
$$\kappa = 43{,}827(SG)^{1.01} \quad \text{for poplar}$$
$$(r^2 = 0.32 \text{ for transformed linear model}) \quad (15)$$

with mean KPERR of 1.99% and 0.92% on the overprediction side for pine and poplar, respectively. The pine model has a maximum overprediction error of 69% and maximum underprediction error of 33%; that for poplar has maximum overprediction of 39% and maximum underprediction of 19%. The addition of either block shear strength or perpendicular-to-grain tensile strength to the model did not provide any substantial improvement in predictive ability. This may be partly attributed to the differences in the stresses induced at the notch and the stresses measured and computed using standard ASTM clear specimen tests for block shear strength and perpendicular-to-grain tensile strength. The most predominant characteristic that influenced notched beam strength is growth ring orientation and, to some extent, grain angle. These growth characteristics, however, are difficult to control; but limits and worst case conditions could be used to extend the prediction models to design criteria. At present, Eq. (15) is not recommended for predicting κ.

The *preferred* way to establish κ for other materials is by notched beam tests. A random sample of beams can be collected from a given species. κ is determined by destructive testing of TEN beams with the notch located at $M/V \geq 10.0$ in. to match the κ in this work. All other notch and beam geometry variables can be arbitrarily selected but should be varied for wide applicability and smoothing of minor effects. With adequate sample size, appropriate statistical properties of the κ distribution can be determined. An allowable value can be established for each species by modifying the lower 5% exclusion limit, similar to current practice for deriving allowable unit stresses of visually graded structural lumber.

CONCLUSIONS

Critical fillet hoop stress (CFHS) theory was successfully used to develop an equation for predicting the strength of tension end-notched (TEN) wood beams. The equation combines the results of finite element and statistical analyses of 690 different TEN beam configurations and experimental tests of 362 full-size beams. This closed-form expression accounts for the effects of loading type, end support, and beam and notch geometry variables such as beam height, fractional notch depth, radius, and notch location. The effect of span-to-depth ratio is implicit to the model. Notched beam strength is represented by a material parameter, κ, which can be obtained by destructive testing of notched beams.

The strength equation applies to both filleted and sharp-cornered tension end notches. An effective radius, R_e, is used to model a sharp-cornered notch ($R \simeq 0$); R_e was determined and confirmed for two materials. A method of determining R_e for other materials was shown.

This equation can be used to establish design criteria for notched beams that explicitly consider notch geometries and the relative proportion of moment and shear at the notch sections. These factors are currently not considered by designers.

ACKNOWLEDGMENTS

The authors thank Dr. Panickos Palettas of Virginia Tech's Statistical Consulting Center for his assistance in statistical design and analysis. In addition, we appreciate the finite element mesh generator program written by Dr. Barry Zalph, who also gave many invaluable comments over the course of the study. This research was supported, in part, by the USDA Competitive Grants Program for Forest and Rangeland Renewable Resources.

REFERENCES

Abou-Ghaida, S., and V. K. A. Gopu. 1984. Shear strength in notched timber beams. Pages 579–586 *in* Proc. Pacific Timber Engineering Conf., May 1984, Auckland, New Zealand.

American Institute of Timber Construction. 1985. Timber construction manual, 3rd ed. John Wiley and Sons, New York, NY.

American Society for Testing and Materials. 1988. Annual book of ASTM standards, vol. 4.09, Wood. ASTM, Philadelphia, PA.

Bendtsen, B. A., and S. Porter. 1978. Comparison of results from standard 2-inch width 1½-inch shear block tests. Forest Prod. J. 28(7):54–56.

Choi, I., and C. O. Horgan. 1977. Saint-Venant's principle and end effects in anisotropic elasticity. J. Appl. Mechanics 14(Sep.):424–430.

Cook, R. D., and W. C. Young. 1985. Advanced mechanics of materials. Macmillan Publishing Co., New York, NY.

CSA. 1989. Engineering design in wood (limit states design). CAN3-086.1-M89, Canadian Standards Association.

Foliente, G. C. 1989. Predicting strength of wood beams with tension end notches. M.S. thesis, Virginia Polytechnic Institute and State University, Blacksburg, VA.

———, and T. E. McLain. 1991. Design of notched wood beams. Pages 64–67 *in* Proc. ASCE Structures Congress '91, 29 April–01 May 1991, Indianapolis, IN.

Gerhardt, T. D. 1983. Plane stress analysis of wood members using isoparametric finite elements: A computer program. US Forest Service General Technical Report FPL 35. Madison, WI. 15 pp.

———. 1984a. Strength and stiffness analysis of notched green oak pallet stringers. US Forest Service Research Paper FPL 452. Madison, WI. 25 pp.

———. 1984b. A hybrid/finite element approach for stress analysis of notched anisotropic materials. J. Appl. Mechanics 51(Dec.):804–810.

Gustafsson, P. J. 1988. A study of strength of notched beams. Paper CIB-W18A/21-10-1. Intl. Council for Bldg. Research Studies and Documentation, Vancouver, B.C., Canada. 25 pp.

Hirai, T., and M. Sawada. 1979. Stiffness and load carrying capacity of square-notched beams, 1: On the estimation of the effective stiffness. Research Bulletins of the College Experiment Forests, College of Agriculture, Hokkaido University 36(2):387–420, Sapporo, Japan.

Horgan, C. O. 1982. Saint-Venant end effects in composites. J. Composite Materials 16(Sep.):411–421.

Leicester, R. H., and W. G. Poynter. 1979. On the design strength of notched beams. Proc. 19th For. Prods. Res. Conf., 12–16 November 1979, Melbourne, Australia.

Mettem, C. J. 1986. Structural timber design and technology. Longman Scientific and Technical, Essex, England.

Murphy, J. F. 1978. Using fracture mechanics to predict failure in notched wood beams. Pages 159–173 *in* Proc.

First Intl. Conf. Wood Fracture, Aug. 1978, Banff, Alberta, Canada.

———. 1986. Strength and stiffness reduction of large notched beams. J. Structural Engineering 2(9):1989–2000.

NFPA. 1986. National design specification for wood construction. National Forest Products Association, Washington, DC. 87 pp.

SAA. 1988. Australian standard 1720.1-1988: SAA timber structures code, Part 1—Design methods. Standards Association of Australia, Sydney, Australia. 85 pp.

SANDORFF, P. E. 1980. Saint-Venant effects in an orthotropic beam. J. Composite Materials 14(July):199–212.

SAS INSTITUTE. 1985. SAS user's guide: Statistics. Version 5 Edition. SAS Institute Inc., Cary, NC.

SCHOLTEN, J. A. 1935. Rounding notches makes stronger joists. American Lumberman, March 1935.

STIEDA, C. K. A. 1966. Stress concentrations around holes and notches and their effect on the strength of wood beams. J. Materials 1(3):560–582.

USDA. 1987. Wood handbook: Wood as an engineering material. USDA Agric. Handbook No. 72. US Forest Products Laboratory, Madison, WI. 466 pp.

WALSH, P. F. 1972. Linear fracture mechanics in orthotropic materials. Engineering Fracture Mechanics 4:533–541.

ZALPH, B. L. 1989. Predicting the strength of notched wood beams. Ph.D. dissertation, Virginia Polytechnic Institute and State University, Blacksburg, VA.

———, AND T. E. MCLAIN. 1992. Strength of wood beams with filleted interior notches: A new model. Wood Fiber Sci. 24(2):204–215.